



Copper-doped sulfonic acid-functionalized MIL-101(Cr) metal–organic framework for efficient aerobic oxidation reactions

Xiujuan Li¹ | Zihao Zhou¹ | Yuzhen Zhao² | Daniele Ramella³ | Yi Luan^{1,2}

¹School of Materials Science and Engineering, University of Science and Technology Beijing, 30 Xueyuan Road, Haidian District, Beijing, 100083, China

²Key Laboratory of Organic Polymer Photoelectric Materials, School of Science, Xijing University, Xi'an, Shaanxi Province, 710123, China

³Department of Chemistry, Temple University-Beury Hall, 1901, N. 13th Street Philadelphia, PA, 19122, USA

Correspondence

Yi Luan, School of Materials Science and Engineering, University of Science and Technology Beijing, 30 Xueyuan Road, Haidian District, Beijing 100083, China.
Email: yiluan@ustb.edu.cn

Funding information

Natural Science Basic Research Plan in Shaanxi Province of China, Grant/Award Numbers: No. 2017JM5134, No. 2018JM5047, No. 2018JQ5028, 2018JM5047, 2017JM5134, 2018JQ5028; Natural Science Foundation of Beijing Municipality, Grant/Award Numbers: 2172037, L182020; Beijing Natural Science Foundation, Grant/Award Numbers: L182020, 2172037

A series of Cr-based metal–organic framework MIL-101-SO₃H bearing sulfonic acid functional groups were utilized for the immobilization of catalytically active copper species via a post-synthetic metalation method. The novel materials were fully characterized by scanning electron microscopy, X-ray diffraction, energy dispersive X-ray spectroscopy (EDX), X-ray photoelectron spectroscopy (XPS), the Brunauer–Emmett–Teller method, and thermogravimetric analysis. XPS and the EDX element map both suggested that Cu²⁺ is coordinately bonded to the MIL-101-SO₃H, which forms the MIL-101-SO₃@Cu structure. The obtained copper-doped MIL-101-SO₃@Cu-1, MIL-101-SO₃@Cu-2, and MIL-101-SO₃@Cu-3 catalysts were utilized in the selective oxidation of alcohols and epoxidation of olefins using molecular oxygen as an oxidant. Catalytic aerobic oxidation optimization showed that MIL-101-SO₃@Cu-1 is the optimal catalyst and it can be reused ten times without compromising the yield and selectivity.

KEY WORDS

metal–organic framework, heterogeneous catalyst, copper (II) catalyst, epoxidation reaction, selective alcohol oxidation

1 | INTRODUCTION

Aerobic oxidation reactions are an important class of reactions carried out in industry and widely used in the production of fine chemicals,^[1,2] pharmaceuticals,^[3] and food additives.^[4] Many homogenous catalyst systems have been developed, but most of those methods suffer from problems, including difficulty in recovering the catalyst, and generation of harmful by-products.^[5] As a result, it is important to develop a fast and efficient heterogeneous oxidation catalytic system to

address these issues. General catalytic oxidation processes require the use of large amounts of inorganic oxidants, such as chromium compounds and permanganates, which are toxic and expensive.^[6] Serious environmental problems have led to the development of molecular oxygen as the oxidant source in order to minimize chemical waste.^[7,8] The use of heterogeneous catalysis and molecular oxygen in oxidation reactions provides a green alternative to traditional toxic chemical oxidants.^[9] Extensive research has been carried out to explore efficient catalytic systems for aerobic

oxidation reactions. Transition metals, including Pd,^[10] Ru,^[11] Mn,^[12] Co,^[13] Zn,^[14] Fe,^[15] and Cu,^[16] have been developed to promote aerobic oxidation reactions.^[17] Copper is abundant, inexpensive, environmentally friendly, and relatively high catalytic efficiency.

Several copper catalysts have been developed for aerobic oxidation reactions such as Cu(OTf)/TEMPO,^[18] Cu/TEMPO,^[19] and Cu/DBED.^[20] Copper *p*-toluenesulfonates are homogeneous complexes commonly used as Lewis acid catalysts in organic synthesis; they show low toxicity, moisture tolerance, and reusability.^[21] A combination of copper ions and *p*-toluenesulfonate displayed good aerobic oxidation activity during our preliminary study.^[22] However, these homogeneous copper catalysts are difficult to separate and recover from the reaction system. Heterogeneous copper catalysts have been used to overcome these issues and some heterogeneous copper catalysts have been reported, such as MCM-41-bpy-CuI,^[23] CuTSPc@3D-(N)GFs,^[24] PS/PANI@Cu(OSO₂CF₃)₂,^[25] Cu/MOF,^[26] PVA-stabilized copper oxide nanoparticles,^[27] copper-based coordination polymers,^[28] copper nanoparticles,^[29] and Cu/graphene.^[30] However, some catalytic systems still suffer from instability, the need for harsh reaction conditions, or low utilization of catalytically active metal.

Metal-organic frameworks (MOFs) have attracted considerable interest as highly efficient heterogeneous catalysts due to their unique crystalline porosity, ability to be tailored to need, and ultra-high specific surface area.^[31] As coordination polymers built up from various organic linkers and inorganic connectors,^[32] they are an attractive prospect in heterogeneous catalysis.^[33,34] Several MOF catalysts have been utilized in aerobic oxidation reactions,^[35] including copper-based,^[36] nickel-based,^[37] iron-based,^[38] zinc-based,^[39] chromium-based,^[40] cobalt-based,^[41] and zirconium-based^[42,43] catalysts. Sulfonic acid-based MOFs can be utilized as

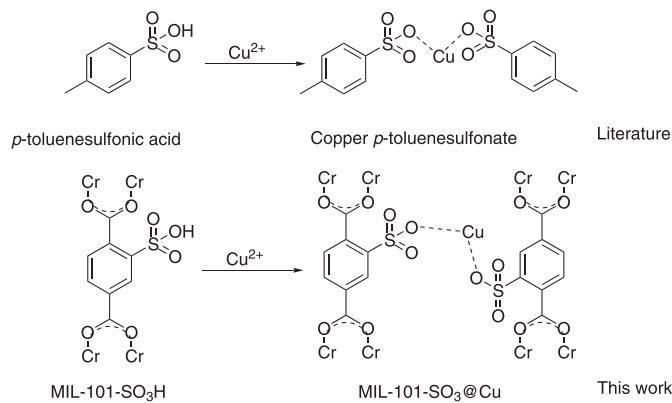
heterogeneous supports thanks to their large surface area and highly porous structure.^[44] Inspired by the unique structure of sulfonic acid MOFs and the synthesis of copper *p*-toluenesulfonate, we focused on introducing copper ions to the sulfonic acid group of the MOF, as shown in Scheme 1.

In this work, we report a copper-immobilized MOF catalyst that enables the development of efficient heterogeneous catalysis. A Cr-based metal-organic framework with sulfonic acid functional groups was synthesized through a simple solvothermal method, incorporating copper ions to form MIL-101-SO₃@Cu. The synthesized MIL-101-SO₃@Cu catalyst served as an efficient catalyst for aerobic oxidation using molecular oxygen (O₂) as an oxidant. Great yields and selectivities were obtained utilizing one of the as-synthesized heterogeneous copper catalysts, MIL-101-SO₃@Cu-1. Furthermore, the turnover number was up to 99 under the optimized reaction conditions. The sulfonic group of MIL-101-SO₃H bonded to Cu²⁺, which stabilizes the catalytically active site. This sulfonic acid stabilizing strategy provided a novel copper catalytic system with high oxidation efficiency and high catalytic recyclability.

2 | EXPERIMENTAL

2.1 | Materials

2-Sulfoterephthalic acid and chromium trioxide were purchased from Alfa Aesar. Copper sulfate pentahydrate (CuSO₄·5H₂O), copper nitrate trihydrate (Cu(NO₃)₂·3H₂O), copper dichloride dihydrate (CuCl₂·2H₂O), and acetonitrile were purchased from the Beijing Chemical Reagent Company. All reagents used in analytical grade were used as received without further purification.



SCHEME 1 The synthesis of copper *p*-toluenesulfonate and MIL-101-SO₃@Cu

2.2 | Preparation of MIL-101-SO₃H

MIL-101-SO₃H was prepared by solvothermal reaction according to the literature.^[45] In a typical procedure, CrO₃ (2.50 g, 25.0 mmol), 2-sulfoterephthalic acid mono-sodium salt (6.70 g, 25.0 mmol), and HF (16 mmol 40 wt%) were mixed with 25 ml of deionized water in a 50-ml round-bottomed flask and stirred for 15 min at room temperature. The solution was then transferred into a Teflon-lined stainless-steel autoclave. The mixture was allowed to react in an oven at 180°C for 24 hr. The obtained green powder was treated in a solution of diluted HCl (0.08 M in methanol and water) and washed with a methanol/water mixture three times to remove additional HCl. Finally, the sample of MIL-101-SO₃H was obtained after 6 hr in a vacuum desiccator at 150°C.

2.3 | Preparation of MIL-101-SO₃@cu catalyst

To a 100-ml round-bottomed flask, MIL-101-SO₃H (0.16 g, 0.18 mmol), Cu (NO₃)₂·3H₂O (0.043 g, 0.18 mmol), and 50 ml of ethanol were added. The mixture was stirred at 60°C for 12 hr. Subsequently, the solid was separated by centrifugation and washed by a 1:1 mixture of water and ethanol for three times. Then it was washed once by acetonitrile and dried. Finally, the catalyst MIL-101-SO₃@Cu-1 was obtained as solid powder. Similar standard procedures were used for the synthesis of MIL-101-SO₃@Cu-2 from CuCl₂·2H₂O (0.03 g, 0.18 mmol) and MIL-101-SO₃@Cu-3 from CuSO₄·5H₂O (0.045 g, 0.18 mmol).

2.4 | Material characterization

Scanning electron microscopy (SEM) images of samples were obtained with a ZEISS SUPRA 55. Energy dispersive X-ray spectroscopy Energy Dispersive X-Ray (EDX) elemental maps were obtained using a VEGA TS 5130 LM (Tescan). Transmission electron microscopy (TEM) images were revealed by a JEOL JSM-6700. The Langmuir surface area (Brunauer–Emmett–Teller [BET] method), pore volume, and pore diameter were measured by an AUTOSORB-1C analyzer. The phase composition of the products was characterized by X-ray powder diffraction (XRD, Cu K α radiation, $\lambda = 0.1542$ nm) via a M21X diffractometer. Fourier transform infrared spectra were collected by a Nicolet 6700 spectrometer. X-ray photoelectron spectroscopy (XPS) data were obtained using a Shimadzu ESCA-3200. Thermogravimetric analysis (TGA) was performed using an STA 449F3 instrument

under nitrogen flow. The metal copper ion loadings of the catalyst were analyzed using inductively coupled plasma-atomic emission spectrometry (ICP-AES) on a Varian 715-ES. The catalytic reaction product profile was analyzed using a gas chromatography-mass spectrometer (GC-MS, Agilent7890/597 5C-GC/MSD), and nitrobenzene was employed as the internal standard.

2.5 | Catalytic test

2.5.1 | Aerobic oxidation of alcohols

MIL-101-SO₃@Cu catalyst (1.0 mol% based on copper content), NaHCO₃ (1.0 mmol), TEMPO (0.5 mmol), and alcohols (1.0 mmol) were added to solvent (5.0 ml). The reaction was purged three times with oxygen gas, which was supplied through a balloon, and stirred at 60°C for 6 hr. The supernatant was analyzed by GC-MS using nitrobenzene as the internal standard.

2.5.2 | Epoxidation of olefins

Generally, the catalytic reaction was carried out under the following conditions. MIL-101-SO₃@Cu catalyst (1.0 mol% based on copper content), the substrate (1.0 mmol), and pivalaldehyde (1.2 mmol) were mixed in acetonitrile (5.0 ml). The reaction mixture was purged with oxygen gas that was supplied through a balloon and stirred at 40°C for 4 hr. After each catalytic cycle, the solution was centrifuged and the filtered liquid solution was analyzed via GC-MS using nitrobenzene as the internal standard.

2.6 | Recyclability experiment

Under optimal reaction conditions, the selective epoxidation of cyclooctene was examined using the recovered MIL-101-SO₃@Cu-1 catalyst. The catalyst was filtered off, washed with ethanol for three times, and then dried. Finally, it was reused for the next round of catalytic oxidation.

2.7 | Leaching test

The standard catalytic epoxidation of cyclooctene was carried out using the above method. After 1 hr, the MIL-101-SO₃@Cu-1 was separated from the reaction mixture by centrifugation and the supernatant liquid was analyzed by GC-MS. The obtained supernatant was then

directly stirred for an additional 3 hr and analyzed by GC-MS. A comparison of the results of these two GC-MS reactions provides evidence for the leaching of copper from MIL-101-SO₃@Cu-1 catalyst.

3 | RESULTS AND DISCUSSION

3.1 | Characterization of the MIL-101-SO₃@Cu catalyst

As shown in Scheme 2, the Cr-based MOF with sulfonic acid functional groups (MIL-101-SO₃H) was synthesized using the solvothermal method according to the literature report,^[46] followed by post-synthesis modification with copper salts to obtain MIL-101-SO₃@Cu. The variation of MIL-101-SO₃@Cu catalyst was synthesized on treatment with different copper salts. MIL-101-SO₃@Cu-1, -2, and -3 correspond to the Cu (NO₃)₂·3H₂O, CuCl₂·2H₂O, and CuSO₄·5H₂O salts, respectively.

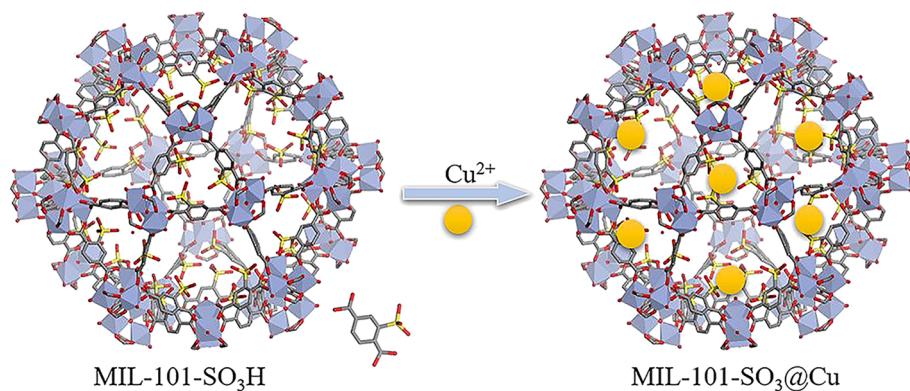
The structural model of MIL-101-SO₃@Cu was built under the Materials Studio package. The state of the copper ion is also demonstrated in Figure 1 after molecular

optimization. The distance between Cu and O was measured to be 1.70 Å and the angle of the O-Cu-O bonds were measured to be 140.1°.

The fractions of the copper species in the MOFs for MIL-101-SO₃@Cu-1, -2, and -3 were determined to be 2.04, 1.59, and 2.58 wt% measured by ICP-AES. MIL-101-SO₃@Cu-1 was the optimal heterogeneous copper catalyst according to the benzyl alcohol oxidation evaluations in Table 1. As a result, MIL-101-SO₃@Cu-1 was chosen for further material characterizations.

The crystalline structures of MIL-101-SO₃H and MIL-101-SO₃@Cu-1 were evidenced by SEM and are shown in Figure 2. MIL-101-SO₃H crystals appear to form a typical cage structure in Figure 2a and the structural morphology was maintained after the immobilization of catalytically active Cu²⁺, as shown in Figure 2b. The crystals of MIL-101-SO₃H are evenly distributed with a size of about 200 nm.

In order to analyze the elemental distribution of MIL-101-SO₃@Cu-1, we performed EDX imaging and spectral measurements, as shown in Figure 3. The EDX elemental map results verified the successful incorporation of Cu²⁺. In addition, EDX showed that the copper was well dis-



SCHEME 2 Schematic illustration of MIL-101-SO₃@Cu synthesis

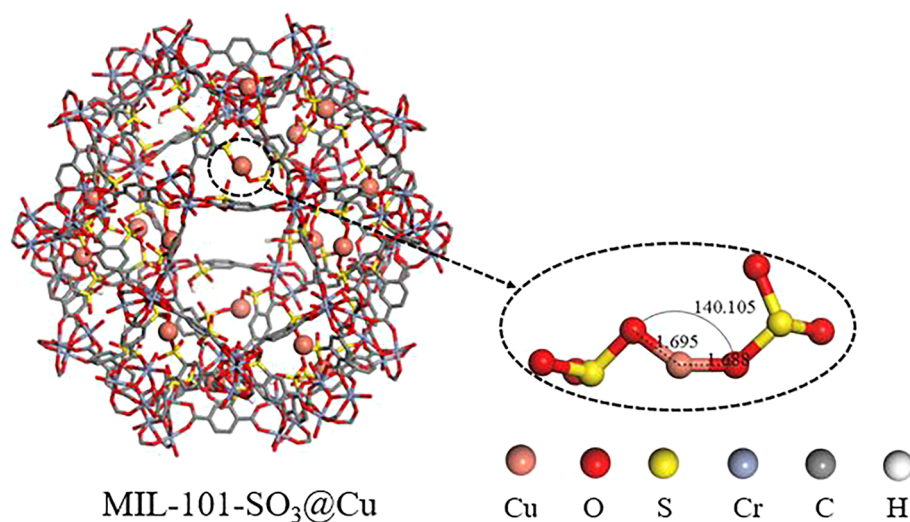


FIGURE 1 Illustration of copper on MIL-101-SO₃Cu. The geometry optimization was performed using the Materials Studio package

TABLE 1 Aerobic oxidation of benzyl alcohol under various reaction conditions^a

Entry	Catalyst	Solvent	Con.	Sel.
			(%) ^b	(%) ^b
1	–	Acetonitrile	<5%	>99
2	MIL-101	Acetonitrile	<5%	>99
3	MIL-101-SO ₃ H	Acetonitrile	<10%	>99
4	MIL-101-SO ₃ @Cu-1	Acetonitrile	>99	>99
5	MIL-101-SO ₃ @Cu-2	Acetonitrile	83	>99
6	MIL-101-SO ₃ @Cu-3	Acetonitrile	90	>99
7	Cu (NO ₃) ₂ ·3H ₂ O	Acetonitrile	87	>99
8	Cu (NO ₃) ₂ ·3H ₂ O ^c	Acetonitrile	99	>99
9	CuSO ₄ ·5H ₂ O	Acetonitrile	43	>99
10	CuCl ₂ ·2H ₂ O	Acetonitrile	68	>99
11	MIL-101-SO ₃ @Cu-1	Ethanol	89	>99
12	MIL-101-SO ₃ @Cu-1	Acetone	74	>99
13	MIL-101-SO ₃ @Cu-1	THF	18	>99
14	MIL-101-SO ₃ @Cu-1	Toluene	46	>99

^aReaction conditions: benzyl alcohol (1.0 mmol), catalyst (based on 1.0 mol% copper, NaHCO₃ (1.0 mmol), TEMPO (0.5 mmol), solvent (5.0 ml), O₂ (1.0 atm), 60°C, 6 hr.

^bDetermined by GC-MS using nitrobenzene as the internal standard.

^cReaction conditions: benzyl alcohol (1.0 mmol), catalyst (based on 9.0 mol% Cu (NO₃)₂·3H₂O, NaHCO₃ (1.0 mmol), TEMPO (0.5 mmol), solvent (5.0 ml), O₂ (1.0 atm), 60°C, 6 hr.

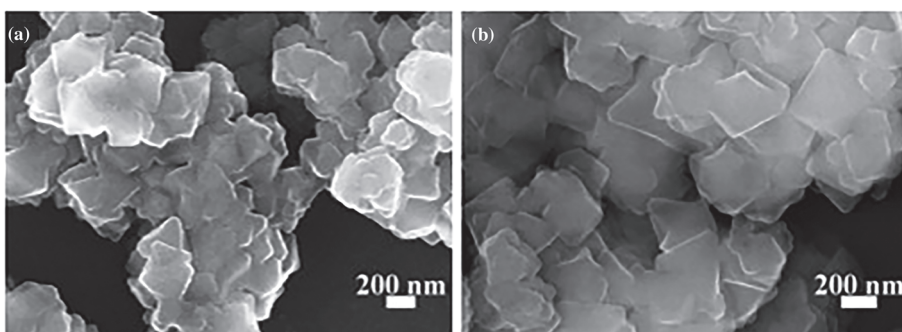
persed in and on the surface of MIL-101-SO₃H. This observation fits our expectation that the copper(II) sites are evenly distributed on the heterogeneous support.

The structural integrity of the MIL-101-SO₃H and MIL-101-SO₃@Cu-1 catalysts was proved by powder X-ray diffraction (PXRD) (Figure 4). The PXRD spectrum revealed the great crystalline structure of MIL-101-SO₃H and the character diffraction peaks of MIL-101 were

found at $2\theta = 2.82, 8.45$, and 16.90 , which is in agreement with the literature report (Figure 4a).^[47] The PXRD pattern for MIL-101-SO₃@Cu-1 (Figure 4c) indicates that -MIL-101 (Figure 4a) and MIL-101-SO₃H (Figure 4b) have a high degree of similarity in terms of the main framework, formed by a chromium cluster and 2-sulfoterephthalic acid ligands.

The Fourier transform infrared spectra of MIL-101-SO₃H and MIL-101-SO₃@Cu-1 are compared in Figure 5. The peaks at 621 cm^{-1} (a) and 624 cm^{-1} (b) can be assigned to C-S stretching vibrations.^[48] The peak at 1025 cm^{-1} can be attributed to the S-O stretching vibration. The peaks at 1180 cm^{-1} and 1224 cm^{-1} (a), and 1184 cm^{-1} and 1225 cm^{-1} (b) correspond to O=S=O symmetric and asymmetric stretching.^[49] For MIL-101-SO₃@Cu-1, a new peak appears at 607 cm^{-1} , which can be attributed to the vibration mode of Cu-O.^[50] There is no peak around 607 cm^{-1} in the Fourier transform infrared spectroscopy (FT-IR) pattern of MIL-101-SO₃H, indicating that the Cu²⁺ ion has bonded with O successfully and the strategy of introducing Cu²⁺ into the sulfonic acid group of the MOF is workable.

XPS measurements were performed for MIL-101-SO₃@Cu-1 to further investigate coordination environments. Figure 6a shows the survey XPS data and indicates that MIL-101-SO₃@Cu contains five elements: Cr, O, C, S, and Cu. The Cr 2p_{1/2} and Cr 2p_{3/2} signals show two peaks at 587.4 and 577.7 eV (Figure 6b), respectively. Both peaks corresponded to the typical binding energies of Cr³⁺.^[51] Figure 6c shows the high-resolution Cu 2p spectrum with four peaks. The prominent peaks at 934.1 and 954.7 eV can be ascribed to Cu 2p_{3/2} and 2p_{1/2}, and the other two are satellite peaks.^[52] The four peaks confirm that the valence state of the Cu ions is +2^[53] and the Cu 2p spectrum corresponds closely to the XPS spectrum of CuO,^[54] which means that the Cu and O might be covalently bonded. The S 2p spectrum also splits into two peaks at 168.2 and 169.2 eV (Figure 6d), which could be attributed to S-O and S=O bonds at an intensity ratio of 1:2.^[55] The O 1s spectrum exhibits two oxygen bonding features

**FIGURE 2** SEM images of (a) MIL-101-SO₃H and (b) MIL-101-SO₃@Cu-1

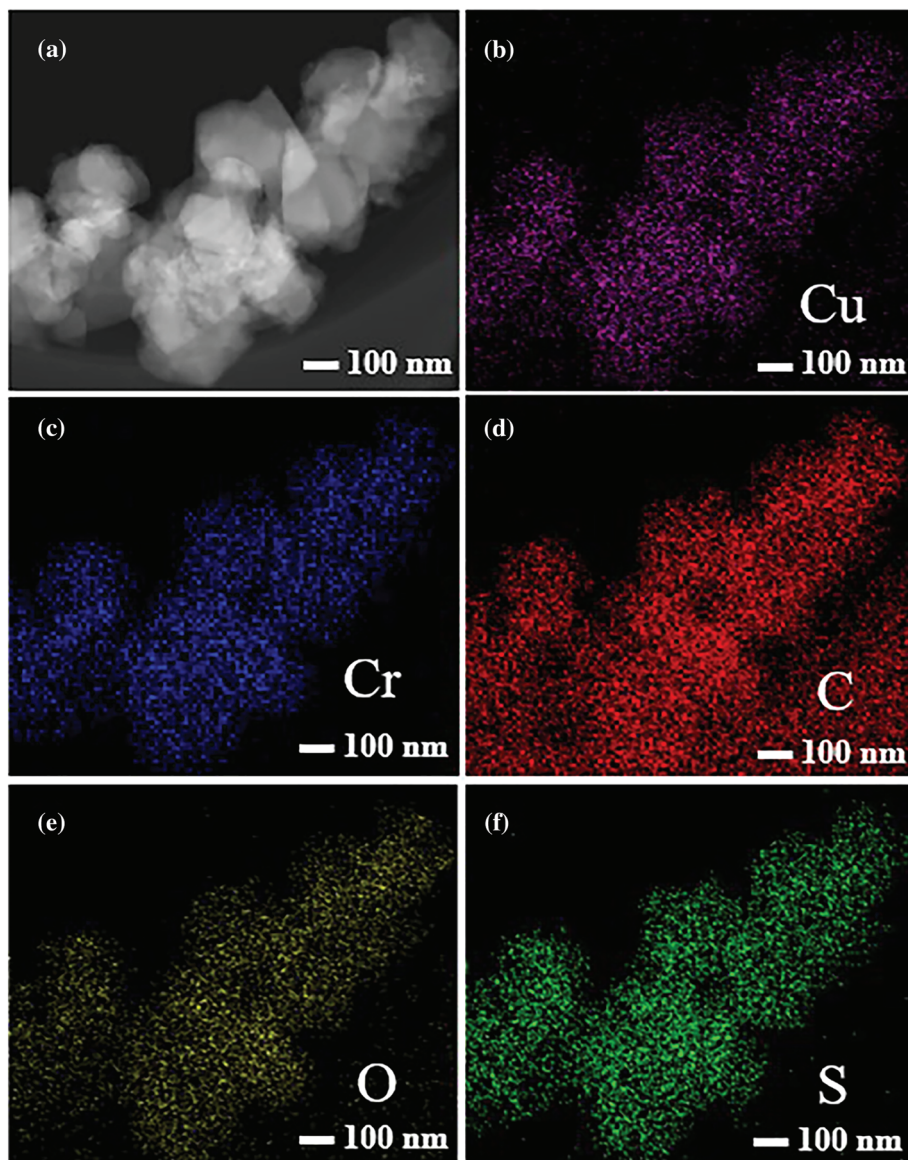


FIGURE 3 (a) TEM images of MIL-101-SO₃@Cu-1 and (b-f) EDX elemental maps of Cu, Cr, C, O, and S

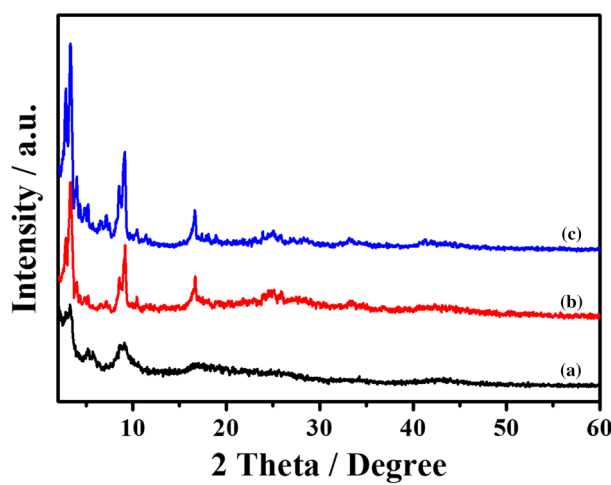


FIGURE 4 XRD patterns of (a) MIL-101, (b) MIL-101-SO₃H, and (c) MIL-101-SO₃@Cu-1

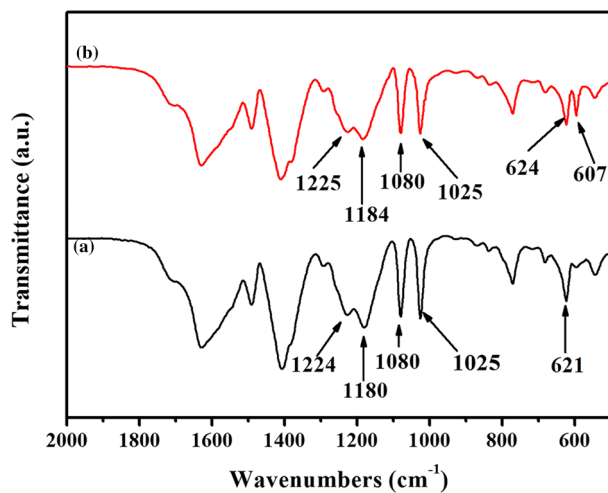
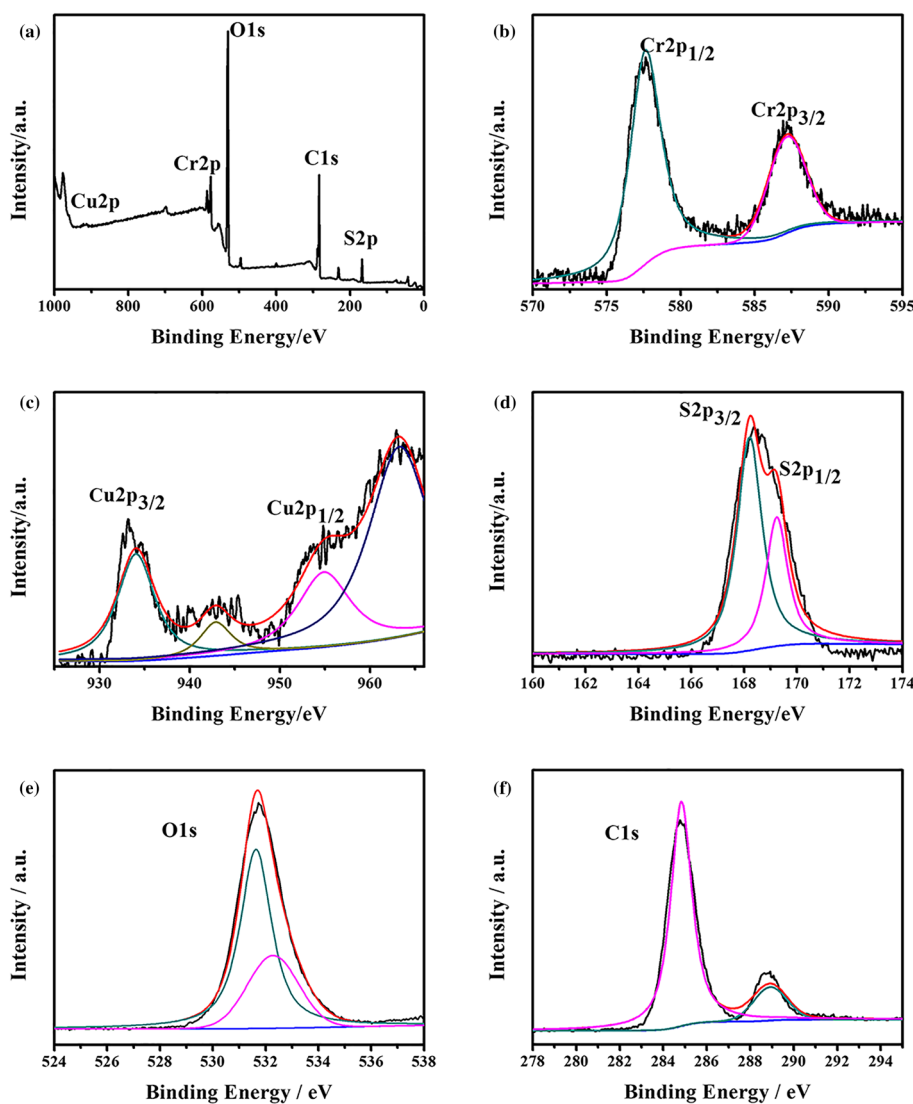


FIGURE 5 FT-IR pattern of (a) MIL-101-SO₃H and (b) MIL-101-SO₃@Cu-1

FIGURE 6 XPS spectra of MIL-101-SO₃@Cu-1: (a) survey spectrum, (b) high-resolution Cr spectrum, (c) high-resolution Cu spectrum, (d) high-resolution S spectrum, (e) high-resolution O spectrum, and (f) high-resolution C spectrum



(Figure 6e). The peak at 531.7 eV is typical of the metal–oxygen bond,^[56] while the peak at 532.3 eV can be attributed to OH groups from the adsorbed H₂O molecules or SO₃H groups. Furthermore, the oxidation state of the copper was confirmed. The C 1 s spectrum in Figure 6f can be divided into two peaks at 284.8 and 289.2 eV, which can be attributed to C=C in aromatic rings and Cr-O-C species.^[57]

The thermal stability of the MIL-101-SO₃H and MIL-101-SO₃@Cu MOF materials was further examined by TGA in the temperature range of 100–800°C (Figure 7). The TGA curve of MIL-101-SO₃H shows no significant changes after incorporation of Cu²⁺. They all show a two-step weight loss which can be attributed to loss of the guest molecules before 300°C and the other significant weight loss after 500°C. The TGA results suggest

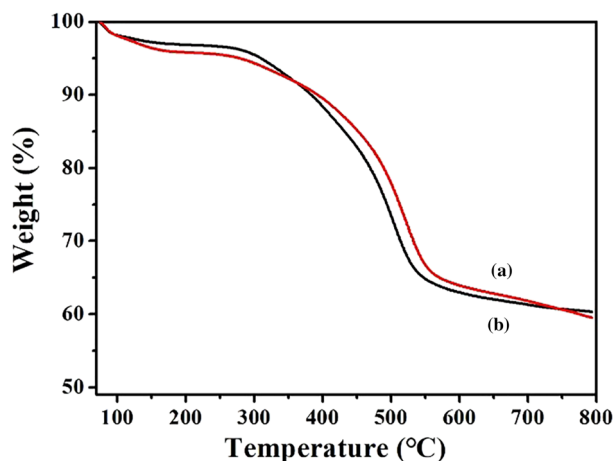


FIGURE 7 TGA of (a) MIL-101-SO₃H and (b) MIL-101-SO₃@Cu-1

that our post-synthesis modification method does not change the thermal stability of the catalyst and the optimal epoxidation catalyst MIL-101-SO₃@Cu can maintain its stability at a temperature of up to 300°C.

The porosity of MIL-101-SO₃@Cu-1 was characterized by the N₂ adsorption-desorption isotherm (Figure 8). Typical type I isotherms of MIL-101-SO₃@Cu-1 were observed, revealing the microporous properties of the material. The surface area of the sample was calculated using the BET method. MIL-101-SO₃@Cu-1 had a BET surface area of 822.438 m²/g, a total microporous volume of 0.37 cm³/g, and a total pore volume of 0.50 cm³/g. In comparison with MIL-101-SO₃H, which has a BET surface area of 1066 m²/g (Figure S1, ESI†), MIL-101-SO₃@Cu-1 showed a slightly decreased surface area because of copper loading.

3.2 | Catalytic activity of MIL-101-SO₃@cu for selective aerobic oxidation

The catalytic abilities of the MIL-101-SO₃@Cu were optimized by employing aerobic benzyl alcohol oxidation as the model reaction. Various catalysts and solvents were evaluated and the results are summarized in Table 1. The aerobic oxidation of benzyl alcohol was carried out in the presence of molecular oxygen as stoichiometric oxidant, together with 0.50 equiv of TEMPO and 1.0 equiv NaHCO₃. A control experiment was performed to study the background rate in the aerobic oxidation of benzyl alcohol (Table 1, entry 1). There was almost no conversion in the absence of catalyst. The MIL-101 and MIL-101-SO₃H catalysts only showed a low yield, which suggests the crucial role of copper in the aerobic oxidation reactions (Table 1, entries 2 and 3). When MIL-101-SO₃@Cu was utilized as the catalyst, the reaction system showed a high conversion owing to the highly

efficient catalytic activity of Cu²⁺ (Table 1, entries 4–6). Among the three catalysts of MIL-101-SO₃@Cu that were found to be catalytically active towards benzyl alcohol, MIL-101-SO₃@Cu-1 (derived from Cu (NO₃)₂·3H₂O) was found to be the optimal catalyst (Table 1, entry 4). Furthermore, the homogeneous Cu (NO₃)₂·3H₂O catalyst showed only modest conversion (Table 1, entry 7) under the same reaction conditions. When 9.0 mol% of the catalyst was used, 99% yield was achieved due to the large excess of the required catalyst (Table 1, entry 8). The other copper salts, CuSO₄·5H₂O and CuCl₂·2H₂O, showed very low conversion (Table 1, entries 9 and 10). In addition, solvent evaluation indicated that acetonitrile is the most suitable reaction solvent for this reaction (Table 1, entries 11–14). Oxygen-containing solvents, such as ethanol (Table 1, entry 11), acetone (Table 1, entry 12), and THF (Table 1, entry 13), showed compromised conversions, probably due to the undesired oxygen coordination. A low-polarity solvent such as toluene, only gave poor yields of the desired product (Table 1, entry 14).

After optimizing our catalytic oxidation reaction, we studied the substrate scope of this methodology (Table 2). Under optimal reaction conditions, the conversion of benzyl alcohol was achieved to be 99%, together with 99% selectivity of benzaldehyde (Table 2, entry 1). Various copper catalysts from literature reports are summarized in Table S1 (ESI†). The synthesized MIL-101-SO₃@Cu-1 catalyst showed one of the best catalytic performance in terms of turnover number and turnover frequency. Electron-rich benzyl alcohols, such as 4-methylbenzyl alcohol and 4-methoxybenzyl alcohol, were converted to the corresponding aldehyde in a yield of 99% (Table 2, entries 2 and 3). In addition, the 4-fluorobenzyl alcohol, which has an electron-withdrawing group at the para position, showed a slightly compromised conversion (Table 2, entry 4) due to the lower electron density on the aromatic ring. The aerobic oxidation of heteroaromatic alcohols was also successful. 2-Pyridinemethanol gave an excellent yield of 2-pyridinealdehyde (Table 2, entry 5). However, 2-thiophenemethanol provided the corresponding thiophene-2-carboxaldehyde with a 69% conversion (Table 2, entry 6). Cinnamyl alcohol had a good yield due to the presence of an electron-rich aromatic ring (Table 2 entry 7). The allylic alcohol 3-methyl-2-but en-1-ol showed a decent conversion and selectivity (Table 2, entry 8). The catalytic oxidation of secondary alcohols such as 1-phenylethanol and cyclohexanol (Table 2, entries 9 and 10) was also investigated. Only poor to modest yields were achieved due to the steric hindrance and electronic effects of the secondary alcohols.

Furthermore, aerobic epoxidation of olefins was also studied in the presence of MIL-101-SO₃@Cu-1 catalyst

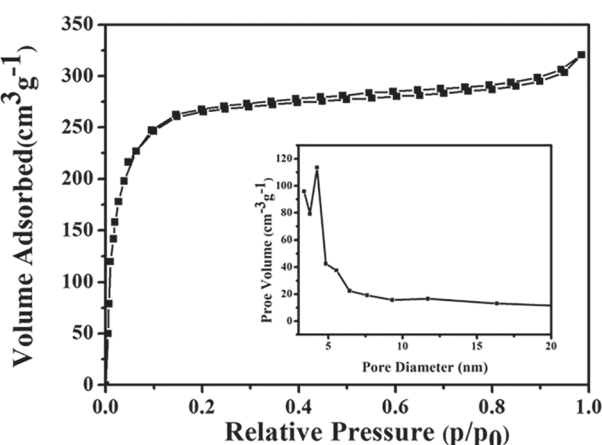


FIGURE 8 N₂ adsorption/desorption of MIL-101-SO₃@Cu-1

TABLE 2 Aerobic oxidation of alcohols catalyzed by MIL-101-SO₃@Cu-1^a

Entry	Substrate	Product	Con. (%) ^b	Sel. (%) ^b
1			>99	>99
2			>99	>99
3			>99	>99
4			91	>99
5			>99	>99
6			69	92
7			>99	>99
8			48	>99
9			55	>99
10			12	>99

^aReaction conditions: alcohol (1.0 mmol), catalyst (based on 1.0 mol% copper), NaHCO₃ (1.0 mmol), TEMPO (0.5 mmol), acetonitrile (5.0 ml), O₂ (1.0 atm), 60°C, 6 hr.

^bDetermined by GC-MS using nitrobenzene as the internal standard.

TABLE 3 Aerobic epoxidation of olefins catalyzed by MIL-101-SO₃@Cu-1^a

Entry	Substrate	Product	Time (h)	Con. (%) ^b	Sel. (%) ^b
1			4	>99	>99
2			4	>99	>99
3			4	>99	>99
4			5	73	>99
5			5	69	>99
6			20	82	85
7			20	>99	>99
8			20	77	>99

^aReaction conditions: olefin (1.0 mmol), MIL-101-SO₃@Cu-1 (based on 1.0 mol% copper), pivalaldehyde (1.2 mmol), acetonitrile (5.0 ml), 1.0 atm O₂ balloon, 40°C.

^bDetermined by GC using nitrobenzene as the internal standard.

(Table 3). The cyclic olefins, such as cyclooctene, cyclohexene, and 2-norbornene, showed great activity with 99% conversion and 99% selectivity under standard

reaction conditions (Table 3, entries 1–3). Literature reported catalysts for the epoxidation of cyclooctene are summarized in Table S2 (ESI†). Our MIL-101-SO₃@Cu-1

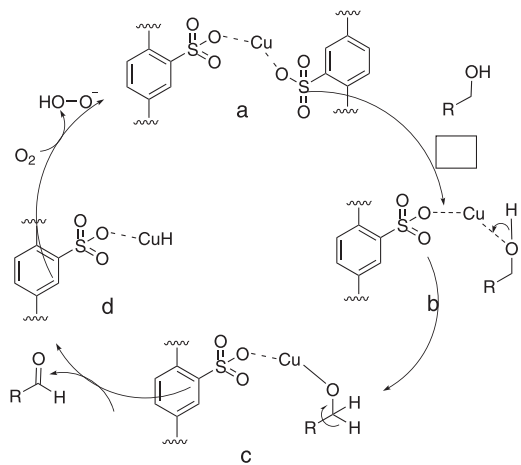
provided a good yield under mild reaction conditions. Low activity can also be observed in linear olefins due to their low electron density (Table 3, entries 4 and 5). 1,2-Dihydronaphthalene was also transformed into its corresponding epoxide in decent conversion and selectivity (Table 3, entry 6). For 1,2-disubstituted aromatic olefins, *trans*-stilbene provided a higher yield than its corresponding *cis*-stilbene due to its steric effect (Table 3, entries 7 and 8).

3.3 | Mechanism of oxidation

The mechanism for MIL-101-SO₃@Cu-catalyzed aerobic oxidation of alcohol under aerobic conditions is described in Scheme 3. In the initial cycle, the alcohol substrate combines with a Cu²⁺ site to form a metal-alkoxide intermediate in order to generate intermediate **b**. An alcohol proton exchange leads to a carbocation intermediate **c**. An oxidative elimination of the proton at alpha position provides the desired aldehyde product, with the generation of intermediate **d**. The regeneration of MOF catalyst **a** is assisted by the oxygen atmosphere.

3.4 | Recyclability of the catalyst

In order to evaluate the recyclability of the MIL-101-SO₃@Cu-1 catalytic material, the catalytic material recovered after the reaction under the foregoing conditions was subjected to epoxidation of cyclooctene again (Figure 9). After each reaction was completed, the catalytic material was separated from the reaction mixture by centrifugation. The MIL-101-SO₃@Cu-1 catalytic material remained catalytically active after each cycle and maintained 99% conversion and 99% selection after



SCHEME 3 Proposed reaction mechanism

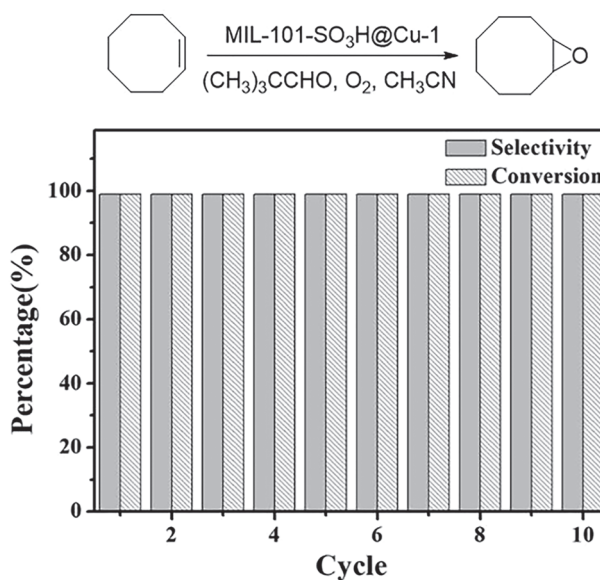


FIGURE 9 The recyclability of MIL-101-SO₃@Cu-1 catalyst in the epoxidation of cyclooctene

ten cycles. The results show that the MIL-101-SO₃@Cu-1 catalytic material exhibits excellent recyclability in the epoxidation of cyclooctene. After ten cycles, the catalyst was assessed by PXRD and the spectrum was similar to that of the fresh catalyst (Figure S2, ESI†), suggesting that the crystalline structure and composition of the MIL-101-SO₃@Cu-1 catalyst were well maintained. Furthermore, the BET surface area of the recycled sample was also measured. A slightly decreased surface area of 805.326 m²/g (Figure S3, ESI†) was found. XPS results indicated that the chemical state of copper and chromium remains unchanged after ten cycles (Figure S4, ESI†).

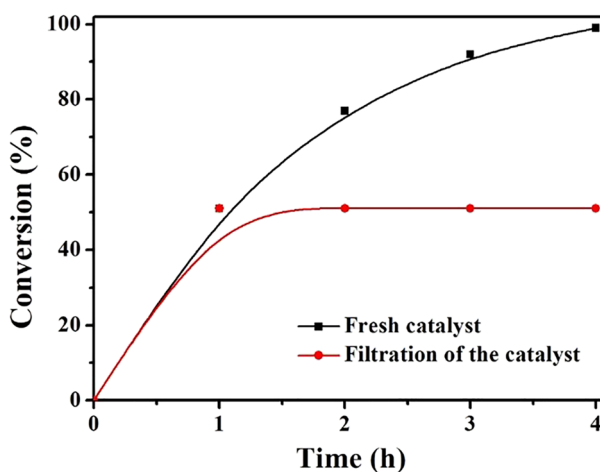


FIGURE 10 The leaching test of MIL-101-SO₃@Cu-1 catalyst in the epoxidation of cyclooctene

3.5 | Leaching test

To verify that copper leaching did not occur during the reaction, epoxidation of cyclooctene was carried out. The catalyst was separated from the catalytic system when the conversion was about 50% after 2 hr (Figure 10). Subsequently, the supernatant was stirred at 40°C for an additional 4 hr. No further conversion of the reactants was observed after removal of the catalytic material. The recyclability of the MIL-101-SO₃@Cu-1 catalyst was also investigated; tests showed excellent performance, as expected (Figure S7 and S8, ESI†). In addition, our ICP-AES analysis of the supernatant mixture showed a copper concentration of only 0.03 ppm, indicating that no significant copper leaching occurred during the reaction; this is likely due to the Cu²⁺ ions being strongly bonded to the O atoms of the sulfonyl groups.

4 | CONCLUSIONS

In summary, a novel MIL-101-SO₃@Cu catalyst has been developed through a simple post-synthetic modification strategy. The structural morphology of MIL-101-SO₃@Cu-1 was fully characterized by SEM, PXRD, XPS, EDX, TGA, FT-IR and BET. The catalyst MIL-101-SO₃ @Cu-1 exhibited excellent catalytic activity; the yield was up to 99% under optimized selective aerobic oxidation conditions. Furthermore, this catalyst could be recycled at least ten times without significant loss of activity and did not suffer from leaching. The excellent thermal stability and high recyclability of the MIL-101-SO₃@Cu-1 catalyst were demonstrated, which take advantage of its covalent bond. This newly developed MIL-101-SO₃@Cu could be further extended to a wide variety of copper-promoted catalytic reactions.

ACKNOWLEDGMENTS

This work was supported by the Beijing Natural Science Foundation (2172037 and L182020) and the Natural Science Basic Research Plan in Shaanxi Province of China (No. 2018JQ5028, No. 2017JM5134 and No. 2018JM5047).

FUNDING INFORMATION

This work was supported by the Beijing Natural Science Foundation (2172037 and L182020) and the Natural Science Basic Research Plan in Shaanxi Province of China (No. 2018JQ5028, No. 2017JM5134 and No. 2018JM5047).

ORCID

Yi Luan  <https://orcid.org/0000-0002-5914-9622>

REFERENCES

- [1] B. S. Lane, K. Burgess, *Chem. Rev.* **2003**, *103*, 2457.
- [2] F. Cavani, J. H. Teles, *ChemSusChem* **2009**, *2*, 508.
- [3] J. L. Everett, J. J. Roberts, W. C. J. Ross, *J. Chem. Soc.* **1953**, 2386.
- [4] P. A. Levene, A. Walti, *J. Biol. Chem.* **1931**, *94*, 367.
- [5] a)S. T. Oyama, *Mechanisms in Homogeneous and Heterogeneous Epoxidation Catalysis*, Elsevier Science **2008**. b)J. Hagen, *Industry Catalysis: A Practical Approach*, Wiley-VCH Verlag GmbH & Co. KGaA, Weinheim 2015.
- [6] C. Parmeggiani, F. Cardona, *Green Chem.* **2012**, *14*(3), 547.
- [7] M. Ueno, S. D. Ohmura, M. Wada, N. Miyoshi, *Tetrahedron Lett.* **2019**, *60*, 570.
- [8] A. Rezaeifard, R. Haddad, M. Jafarpour, M. Hakimi, *J. Am. Chem. Soc.* **2013**, *135*(27), 10036.
- [9] S. E. Davis, M. S. Idea, R. J. Davis, *Green Chem.* **2013**, *15*, 17.
- [10] a)A. V. Iosub, S. S. Stahl, *J. Am. Chem. Soc.* **2015**, *137*, 3454. b) G. Urgoitia, A. Maiztegi, R. SanMartin, M. T. Herrero, E. Dominguez, *RSC Adv.* **2015**, *5*, 103210. c)D. Wang, A. B. Weinstein, P. B. White, S. S. Stahl, *Chem. Rev.* **2018**, *118*(5), 2636.
- [11] a)D. Ventura-Espinosa, C. Vicent, M. Baya, J. A. Mata, *Catal. Sci. Technol.* **2016**, *6*, 8024. b)C. Santilli, I. S. Makarov, P. Fristrup, R. Madsen, *J. Org. Chem.* **2016**, *81*, 9931. c) E. W. Dahl, T. Louis-Goff, N. K. Szymczak, *Chem. Commun.* **2017**, *53*, 2287. d)A. Sarbjana, I. Dutta, P. Daw, S. Dinda, S. M. W. Rahaman, A. Sarkar, J. K. Bera, *ACS Catal.* **2017**, *7*, 2786.
- [12] a)T. Gao, J. Chen, W. Fang, Q. Cao, W. Su, F. Dumeignil, *J. Catal.* **2018**, *368*, 53. b)X. Sun, X. Li, S. Song, Y. Zhu, Y. Liang, N. Jiao, *J. Am. Chem. Soc.* **2015**, *137*, 6059.
- [13] a)W. Partenheimer, V. V. Grushin, *Adv. Synth. Catal.* **2011**, *343*, 102. b)C. W. Anson, S. Ghosh, S. Hammes-Schiffer, S. S. Stahl, *J. Am. Chem. Soc.* **2016**, *138*(12), 4186.
- [14] B. Saha, S. Dutta, M. M. Abu-Omar, *Catal. Sci. Technol.* **2012**, *2*, 79.
- [15] a)T. Taniguchi, H. Ishibashi, *Angew. Chem.* **2013**, *52*(17), 4696. b)T. Hashimoto, D. Hirose, T. Taniguchi, *Adv. Synth. Catal.* **2015**, *357*(14–15), 3346. c)B. Maes, H. Sterckx, C. Sambiagio, F. Lemière, K. Tehrani, *Synlett* **2017**, *28*(13), 1564.
- [16] a)S. D. McCann, S. S. Stahl, *Acc. Chem. Res.* **2015**, *48*(6), 1756. b)S. E. Allen, R. R. Walvoord, R. Padilla-Salinas, M. C. Kozlowski, *Chem. Rev.* **2013**, *113*, 6234. c) A. E. Wendlandt, A. M. Suess, S. S. Stahl, *Angew. Chem. Int. Ed.* **2011**, *50*, 11062. d)H. Zhang, A. W. Schuppe, S. Pan, J. Chen, B. Wang, T. R. Newhouse, L. Yin, *J. Am. Chem. Soc.* **2018**, *140*(15), 5300.
- [17] a)M. Beller, X. F. Wu, XXX, Springer, Berlin/Heidelberg, Germany **2013**. b)F. Yang, B. Zhou, P. Chen, D. Zou, Q. Luo, W. Ren, L. Li, L. Fan, J. Li, *Molecules* **2018**, *23*, 1922.
- [18] B. Sedai, R. T. Baker, *Adv. Synth. Catal.* **2014**, *356*(17), 3563.
- [19] L. Vanoye, M. Pablos, C. Bellefon, A. Favre-Rguillona, *Adv. Synth. Catal.* **2015**, *357*(4), 739.
- [20] B. Xu, J. P. Lumb, B. A. Arndtsen, *Angew. Chem. Int. Ed.* **2015**, *54*, 1.
- [21] M. Wang, Z. Song, H. Gong, H. Jiang, *Synth. Commun.* **2008**, *38*, 961.
- [22] J. Zhao, W. Wang, H. Tang, D. Ramella, Y. Luan, *Mol. Catal.* **2018**, *456*, 57.

- [23] H. Zhao, Q. Chen, L. Wei, Y. Jiang, M. Cai, *Tetrahedron* **2015**, 71, 8725.
- [24] M. Mahyari, M. Sadegh Laeini, A. Shaabani, *Chem. Commun.* **2014**, 50(58), 7855.
- [25] J. Yu, Y. Luan, Y. Qi, J. Hou, W. Dong, M. Yang, G. Wang, *RSC Adv.* **2014**, 4, 55028.
- [26] a)P. Cancino, A. Vega, A. Santiago-Portillo, S. Navalón, M. Alvaro, P. Aguirre, E. Spodine, H. Garcia, *Catal. Sci. Technol.* **2016**, 6, 3727. b)A. Dhakshinamoorthy, M. Alvaro, H. Garcia, *ACS Catal.* **2011**, 1, 48. c)D. Li, Q. Xu, Y. Li, Y. Qiu, P. Ma, J. Niu, J. Wang, *Inorg. Chem.* **2019**, 58, 4945. d) A. Karmakar, M. M. A. Soliman, E. C. B. A. Alegria, G. M. D. M. Rubio, M. F. C. Guedes da Silva, A. J. L. Pombeiro, *New J. Chem.* **2019**, 43, 9843. e)S. Jamalifard, J. Mokhtari, Z. Mirjafary, *RSC Adv.* **2019**, 9, 22749.
- [27] F. P. Silva, R. V. Gonçalves, L. M. Rossi, *J. Mol. Catal. A-Chem.* **2017**, 426, 534.
- [28] L. Asgharnejad, A. Abbasi, M. Najafi, J. Janczak, *J. Solid State Chem.* **2019**, 277, 187.
- [29] a)A. Dutta, M. Chetia, A. A. Ali, A. Bordoloi, P. S. Gehlot, A. Kumar, D. Sarma, *Catal. Lett.* **2019**, 149, 141. b) W. H. Wanna, R. Ramua, D. Jamanchi, Y.-F. Tsai, N. Thiagarajan, S. S.-F. Yu, *J. Catal.* **2019**, 370, 332.
- [30] W. Sun, L. Gao, G. Zheng, *Chem. Commun.* **2019**, 55, 8915.
- [31] a)J. Y. Lee, *Chem. Soc. Rev.* **2009**, 38, 1450. b)B. Li, H. Wen, Y. Cui, W. Zhou, G. Qian, B. Chen, *Adv. Mater.* **2016**, 28, 8819. c)A. Dhakshinamoorthy, M. Alvaro, H. Garcia, *Chem. Commun.* **2012**, 48, 11275.
- [32] a)P. Horcajada, C. Serre, G. Maurin, N. A. Ramsahye, F. Balas, M. Vallet Regí, M. Sebban, F. Taulelle, G. Férey, *J. Am. Chem. Soc.* **2008**, 130, 6774.
- [33] a)J. D. Rocca, D. Liu, W. Lin, *Accounts Chem. Res.* **2011**, 44, 857. b)H. Furukawa, K. E. Cordova, M. O'Keeffe, O. M. Yaghi, *Science* **2013**, 341, 1230444. c)E. Coronado, G. M. Espallargas, *Chem. Soc. Rev.* **2013**, 42, 1525.
- [34] A. H. Chughtai, N. Ahmad, H. A. Younus, A. Laypkov, F. Verpoort, *Chem. Soc. Rev.* **2015**, 44, 6804.
- [35] A. Dhakshinamoorthy, A. M. Asiri, H. Garcia, *Chem. – Eur. J.* **2016**, 22, 8012.
- [36] a)J. Wang, F. Jin, H. Ma, X. Li, M. Liu, J. Kan, G. Chen, Y. Dong, *Inorg. Chem.* **2016**, 55(13), 6685. b)P. Cancino, V. Paredes-García, P. Aguirre, E. Spodine, *Catal. Sci. Technol.* **2014**, 4, 2599. c)A. Dhakshinamoorthy, P. Concepcion, *Chem. Commun.* **2016**, 52, 2725.
- [37] C. Guo, Y. Zhang, Y. Zhang, J. Wang, *Chem. Commun.* **2018**, 54, 3701.
- [38] a)A. Dhakshinamoorthy, M. Alvaro, H. Garcia, *ACS Catal.* **2011**, 1(1), 836. b)D. J. Xiao, J. Oktawiec, P. J. Milner, J. R. Long, *J. Am. Chem. Soc.* **2016**, 138, 14371.
- [39] a)A. W. Stubbs, L. Braglia, E. Borfecchia, R. J. Meyer, Y. Román-Leshkov, C. Lamberti, M. Dincă, *ACS Catal.* **2018**, 8, 596. b)J. Hui, H. Chu, W. Zhang, Y. Shen, W. Chen, Y. Hu, W. Liu, C. Gao, S. Guo, G. Xiao, S. Li, Y. Fu, D. Fan, W. Zhang, F. Huo, *Nanoscale* **2018**, 10, 8772.
- [40] a)D. T. Genna, L. Y. Pfund, D. C. Samblanet, A. G. Wong-Foy, A. J. Matzger, M. S. Sanford, *ACS Catal.* **2016**, 6, 3569. b)B. Li, K. Leng, Y. Zhang, J. J. Dynes, J. Wang, Y. Hu, D. Ma, Z. Shi, L. Zhu, D. Zhang, Y. Sun, M. Chrzanowski, S. Ma, *J. Am. Chem. Soc.* **2015**, 137, 4243. c)
- Y. Fu, Y. Guo, Y. Wang, L. Wang, W. Zhan, G. Lu, *Catal. Sci. Technol.* **2017**, 7, 4136.
- [41] a)O. Pliekhov, O. Pliekhova, U. L. Štangar, N. Z. Logar, *Catal. Commun.* **2018**, 110, 88. b)T. Zhang, Y. Hu, T. Han, Y. Zhai, Y. Zheng, *ACS Appl. Mater. Interfaces* **2018**, 10, 15786.
- [42] a)X. Shu, Y. Yu, Y. Jiang, Y. Luan, D. Ramella, *Appl Organometal Chem.* **2017**, 31, e3862. b)J. Baek, B. Rungtaeweevoranit, X. Pei, M. Park, S. C. Fakra, Y. Liu, R. Matheu, S. A. Alshimimri, S. Alshehri, C. A. Trickett, G. A. Somorjai, O. M. Yaghi, *J. Am. Chem. Soc.* **2018**, 140, 18208.
- [43] a)A. Santiago-Portillo, S. Navalón, M. Alvaro, H. Garcia, *J. Catal.* **2018**, 365, 450. b)P. Neves, A. C. Gomes, T. R. Amarante, F. A. A. Paz, M. Pillinger, *Micropor. Mesopor. Mat.* **2015**, 202, 106.
- [44] X. Zhang, L. Chen, Y. Li, H. Li, Z. Xie, Q. Kuang, L. Zheng, *Dalton Trans.* **2019**, 48, 5515.
- [45] F. Zhang, Y. Jin, Y. Fu, Y. Zhong, W. Zhu, A. A. Ibrahim, M. S. El-Shall, *J. Mater. Chem. A* **2015**, 3, 17008.
- [46] a)G. Akiyama, R. Matsuda, H. Sato, M. Takata, S. Kitagawa, *Adv. Mater.* **2011**, 23, 3294. b)G. Ferey, C. Mellot-Draznieks, C. Serre, F. Millange, J. Dutour, S. Surble, I. Margiolaki, *Science* **2005**, 309, 2040.
- [47] Y. Zhou, Y. Chen, Y. Hu, G. Huang, S. Yu, H. Jiang, *Chem. – Eur. J.* **2014**, 20, 14976.
- [48] X. Zhang, L. Chen, Y. Li, H. Li, Z. Xie, Q. Kuang, L. Zheng, *Dalton Trans.* **2019**, 48, 5515.
- [49] Y. Zang, J. Shi, F. Zhang, Y. Zhong, W. Zhu, *Catal. Sci. Technol.* **2013**, 3, 2044.
- [50] J. Li, Y. Chen, H. Liu, P. Wang, F. Liu, *Energy Fuels* **2013**, 27, 2555.
- [51] H. Khajavi, H. A. Stil, H. P. C. E. Kuipers, *ACS Catal.* **2013**, 3, 2617.
- [52] Y. Zhang, J. Huang, Y. Ding, *Appl. Catal. B-Environ.* **2016**, 198, 447.
- [53] H. Gao, G. Wang, Y. Luan, K. Chaikittikul, X. Zhang, M. Yang, W. Dong, Z. Shi, *CrystEngComm* **2014**, 16, 2520.
- [54] R. P. Vasquez, *Surf. Sci. Spectra* **1998**, 5, 262.
- [55] Y. Jin, J. Shi, F. Zhang, Y. Zhong, W. Zhu, *J. Mol. Catal. A - Chem.* **2014**, 383, 167.
- [56] H. Guo, D. Wang, J. Chen, W. Weng, M. Huang, Z. Zheng, *Chem. Eng. J.* **2017**, 289, 479.
- [57] X. Luo, S. Fu, Y. Du, J. Guo, B. Li, *Micropor. Mesopor. Mat.* **2017**, 237, 268.

SUPPORTING INFORMATION

Additional supporting information may be found online in the Supporting Information section at the end of this article.

How to cite this article: Li X, Zhou Z, Zhao Y, Ramella D, Luan Y. Copper-doped sulfonic acid-functionalized MIL-101(Cr) metal–organic framework for efficient aerobic oxidation reactions. *Appl Organometal Chem.* 2020;e5445. <https://doi.org/10.1002/aoc.5445>